AGU PUBLICATIONS

JGR

Journal of Geophysical Research: Solid Earth

RESEARCH ARTICLE
10.1002/2017JB014154

Special Section:
Gas Hydrate in Porous Media: Linking Laboratory and Field Scale Phenomena

Influence of Fines Content on the Mechanical Behavior of Methane Hydrate-Bearing Sediments

Masayuki Hyodo[1], Yang Wu[1], Koji Nakashima[1], Shintaro Kajiyama[1], and Yukio Nakata[1]

[1]Graduate School of Science and Technology for Innovation, Yamaguchi University, Ube, Japan

Abstract Methane hydrate-bearing sediments with different amounts of fines content and at three densities were artificially prepared under controlled temperature and pressure conditions. The void ratios of specimens after isotropic consolidation tend to decrease with a rise in fines content. The fines particles enter into the pore space between sand grains and densify the specimens. A series of triaxial compression tests were performed to systematically investigate the influences of fines content and density on the shear properties of hydrate-free sediments and methane hydrate-bearing sediments. The test results demonstrate that a rise in fines content within methane hydrate-bearing sediments significantly enhances peak shear strength and promotes dilation behavior. These influences are particularly prominent for specimens at loose packing state. A decrease in void ratio increases the shear strength and stiffness of hydrate-free sediments and methane hydrate-bearing sediments containing fines content of 0% and 8.9%. It is noted that the formation of methane hydrate in samples with varying amounts of fines content increases the stress ratios at the critical state. The addition of fines particles into coarse-grained sand grains alters the internal microstructure of sand matrix and the hydrate formation pattern in the pore space between sand grains and fines particles.

Key Points:
- A series of triaxial compression tests were performed on methane hydrate-bearing sediments and hydrate-free sediments with different amounts of fines content and at three levels of density
- The rise in fines content and decrease in void ratio enhanced the peak shear strength and promoted dilation behavior of methane hydrate-bearing sediments
- The presence of methane hydrate increased the stress ratios at the critical state of methane hydrate-bearing sediments with various amounts of fines content

Correspondence to:
Y. Wu,
yangwuuu0226@hotmail.com

Citation:
Hyodo, M., Wu, Y., Nakashima, K., Kajiyama, S., & Nakata, Y. (2017). Influence of fines content on the mechanical behavior of methane hydrate-bearing sediments. *Journal of Geophysical Research: Solid Earth*, *122*. https://doi.org/10.1002/2017JB014154

Received 1 MAR 2017
Accepted 10 SEP 2017
Accepted article online 14 SEP 2017

1. Introduction

Natural gas hydrates are ice-like crystalline compounds which consist of natural gas and water molecules. They are widely distributed in marine sediments and permafrost regions and regarded as promising future energy sources (Chong et al., 2015; Englezos, 1993; Kvenvolden, 1995; Li et al., 2016; Makogon, 2010; Sloan, 1998; Sloan & Koh, 2007; Waite et al., 2009). Gas production from reservoirs has attracted considerable interest but requires advanced engineering technology due to the complex physical events which occur during gas production. The dissociation of gas hydrate into gas and water in accompaniment with gas extraction reduces the stability of the reservoir and overlying sediment, the production well, and the drilling structure, even giving rise to the possibility of subsidence and subsea slides in marine systems (Jin et al., 2016; Kleinberg et al., 2003; Ning et al., 2012; Nixon & Grozic, 2007; Pauli et al., 2003; Sakamoto et al., 2009; Scholz et al., 2011; Sultan et al., 2010; Xu & Germanovich, 2006). Consequently, a good understanding of the mechanical properties of gas hydrate-bearing sediment is relevant for safely exploiting the methane gas from seabed and developing suitable production methodologies.

Several laboratory studies have been performed by previous researchers to examine the mechanical properties of artificial gas hydrate-bearing sediments. Past studies revealed that the presence of hydrate in a specimen altered the stress-strain response from ductile failure to brittle failure and a rise in hydrate saturation enhanced the shear strength and dilation behavior (Durham et al., 2003; Ebinuma et al., 2005; Grozic & Ghiassian, 2010; Hyodo et al., 2005, 2015; Hyodo, Li, et al., 2013; Hyodo, Yoneda, et al., 2013; Kajiyama et al., 2017; Kajiyama et al., 2017; Masui et al., 2005; Miyazaki et al., 2011; Priest et al., 2015; Winters et al., 2007; Yun et al., 2007). Miyazaki et al. (2011) investigated the geomechanical response of methane hydrate-bearing sands formed with different host sands and noticed that the shear strength and stiffness increased with a rise in the effective confining pressures and methane hydrate saturations. Hyodo, Yoneda, et al. (2013) conducted a series of triaxial tests to comprehensively examine the effects of effective confining pressure, hydrate saturation, density, temperature, and pore pressure on the shear response of methane hydrate-bearing sediments.

In addition, some constitutive models have been proposed to predict the stress-strain relationship of methane hydrate-bearing sediments in the recent decade (Lin et al., 2015; Pinkert et al., 2013; Sánchez et al., 2017; Shen et al., 2016; Uchida et al., 2012). The simulated strengths of the pore-filling and cementing

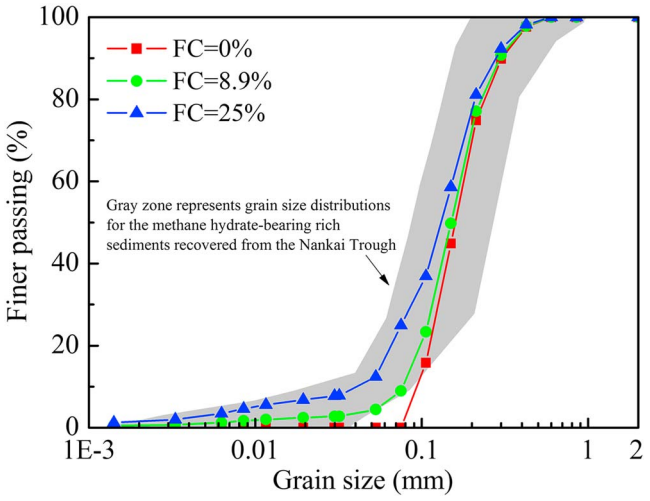

Figure 1. Grain size distribution curves of sands with different amounts of FC.

types of hydrate-bearing sediments classified by Dai et al. (2012) and Waite et al. (2009) were obtained using different values of fitting parameters to interpret the influence of hydrate morphology on the mechanical properties. Brugada et al. (2010); Jung et al. (2012); Shen and Jiang (2016); Xu et al. (2016); and Yu et al. (2016) conducted discrete element modeling to study methane hydrate-bearing sediments using a microscopic contact and bonding method. The majority of the above experimental and numerical investigations were conducted on hydrate-bearing sediments formed with coarse-grained sands without fines content (FC).

However, past studies and field survey data revealed that natural gas hydrate existed in coarse-grained, fine-grained, and fracture-dominated reservoirs (Trehu et al., 2004; Waite et al., 2009). The exploratory test well program (Tokai-oki to kumano-nada) was conducted in the Nankai Trough, offshore Japan, in 2004 and indicated that methane hydrate was mainly concentrated in sand and mud stratified layers with varying grain size distribution curves showing FC in hydrate-bearing sands (Fujii et al., 2005; Minagawa et al., 2008; Suzuki et al., 2009). This is consistent with the investigation results from the offshore gas production test conducted in 2013 (Ito et al., 2015; Santamarina et al., 2015). Marine sediments vary from sandy sediments to clayey-silty sediments with the rise in FC. A rise in FC within the reconstituted marine sediments increases their compressibility and reduces crushability (Hyodo et al., 2017). Some valuable test data on nondestructive pressure core samples containing FC has also been published (Santamarina et al., 2015; Yoneda et al., 2015). The FC in those natural gas hydrate-bearing samples was all less than 10% and the amount could not be controlled or adjusted. Information regarding the quantitative influence of FC on the geomechanical properties of marine sediments containing methane hydrate is still lacking. Therefore, it is necessary to form methane hydrate-bearing sediments with predesignated amounts of FC and test them to clarify the FC impact on geomechanical properties.

A series of triaxial compression tests were performed on synthetic methane hydrate-bearing sediments with varying amounts of FC and at three densities under in situ pressure in this study. The influences of FC and density on the shear strength, stiffness, dilation behavior, and stress characteristics at the critical state were systematically investigated. The shear strengths of methane hydrate-bearing sediments with and without FC are compared under the same test conditions. Finally, a grain-scale microstructure is proposed to interpret the different mechanisms controlling shear behavior of methane hydrate-bearing sediments with and without FC.

2. Materials and Methods

2.1. Test Equipment

An innovative temperature-controlled high-pressure triaxial testing apparatus with the capacity to reproduce subseafloor reservoir conditions is employed in this experimental study. The cell pressure, pore pressure, and temperature could be independently adjusted to simulate in situ conditions. This testing apparatus can provide a maximum axial load up to 200 kN. The designed maximum cell pressure capacity and pore pressure capacity are 30.0 MPa with an accuracy of 0.1 MPa and 20.0 MPa with an accuracy of 0.05 MPa, respectively. The temperature range in the triaxial cell space can vary between −35°C and 30°C. A big external tank for governing the variation in the temperature of specimen is controlled by circulating cell liquid into the triaxial cell space. The cell pressure is supplied by oil pressure and the pore pressure is controlled by upper and lower syringe pumps. The description of this innovative testing apparatus was comprehensively given in previous work (Hyodo, Yoneda, et al., 2013; Hyodo, Li, et al., 2013).

2.2. Materials Tested

Figure 1 shows the grain size distribution curves of tested sands containing different amounts of FC. The gray range represents the grain size distributions of methane hydrate-rich sediments in the Nankai Trough, Japan. One grain size distribution curve with FC of 8.9% by weight within the methane hydrate-rich

Table 1
The Mineralogy Compositions of Host Sediments With Different Amounts of FC

	Small		Median diameter		Large	
Fines content (FC) (%)	Kaolinite	Mica MK 300	Silica sand silt	Silica sand no. 8	Silica sand no. 7	Silica sand R55
0	0.0	0.0	0.0	13.8	75.2	11.0
8.9	1.0	2.0	5.9	12.6	68.5	10.0
25	2.8	5.6	16.7	10.4	56.4	8.2

sediment zones was selected as one of representative host sediments (Suzuki et al., 2009). To quantitatively examine the effect of FC on the shear response of methane hydrate-bearing sediments, grading curves of two other host sediments were artificially prepared through adjusting the amount of FC to 0% and 25%. The grain size distribution curves shift upward with a rise in FC. Table 1 shows the mineralogy compositions of pure host sediments with three amounts of FC. The host sands are composed of silica sands R55, No. 7, and No. 8; silica sand silt; and mica and kaolinite in different proportions by weight. It is in accordance with the mineralogy components of core samples retrieved from the Nankai Trough (Egawa et al., 2015; Ministry of Economy, Trade, and Industry (METI), 2005). Tests on the core samples retrieved from the reservoir in the Nankai Trough indicated that the porosity n varied between 40% and 50% (Suzuki et al., 2009; Yoneda et al., 2015). An energy-controlled tamping method is employed to prepare the specimens with various porosities to be close to the target porosity region. The tamping energy (EC) is determined using equation (1).

$$\mathrm{EC}\,\frac{W_R \cdot H \cdot N_L \cdot N_B}{V} \tag{1}$$

where W_R is the weight of rammer, V is the volume of the mold, H is the rammer drop height, N_L is the total number of tamped layers (N_L = 15 in this study), and N_B is the number of blows for each layer. Three levels of EC of 40 kJ/m^3, 120 kJ/m^3, and 360 kJ/m^3 corresponding to the number of blows N_B of 8, 24, and 72 are applied to attain various porosities.

Table 2
Test Conditions of Triaxial Compression Tests on Methane Hydrate-Bearing Sediments

Test conditions							
FC (%)	*P. P.* (MPa)	*T* (°C)	EC (kJ/m^3)	*n* (%)	*e*	σ_c' (MPa)	S_{MH} (%)
0	10	5	40	48.38	0.94	3	0.0
			40	48.78	0.95		63.1
			120	44.89	0.82		0.0
			120	44.43	0.80		42.2
			360	43.30	0.76		0.0
			360	43.60	0.77		63.3
8.9	10	5	40	48.50	0.94	3	0.0
			40	48.35	0.94		44.0
			120	45.08	0.82		0.0
			120	44.43	0.80		58.9
			360	42.57	0.74		0.0
			360	42.12	0.73		46.1
25	10	5	40	45.18	0.82	3	0.0
			40	44.44	0.80		54.4
			120	41.88	0.72		0.0
			120	42.03	0.73		45.9
			360	40.90	0.67		0.0
			360	39.49	0.65		51.0

Note. FC: fines content, *P. P.*: pore pressure, *T*: temperature, EC: tamping energy, *n*: porosity, *e*: void ratio, σ_c': effective confining pressure, S_{MH}: methane hydrate saturation.

The formation procedure of methane hydrate-bearing sediments is briefly described here. Methane hydrate was formed by a partial water saturation method which was employed in previous studies (Ebinuma et al., 2005; Kneafsey et al., 2007; Masui et al., 2005; Miyazaki et al., 2012; Priest et al., 2006; Waite et al., 2004). The unsaturated specimens containing different amounts of FC were initially prepared by adding a specific water content into the pure sand and sand-silty mixture to attain the target methane hydrate saturation S_{MH} = 50%. The final methane hydrate saturation was experimentally measured after testing. The cylindrical specimen was 60 mm in height and 30 mm in diameter. The moist soil was poured into the mold in 15 layers, compacted using the number of blows N_B corresponding to the given magnitude of EC required to adjust the porosity. The mold restraining the moist specimen was moved into a freezer to freeze the specimen, which allowed the specimen to stand by itself. Subsequently, the frozen specimen was removed from the mold and placed on a pedestal in the triaxial cell room and then covered by butyl rubber. The cell pressure and pore pressure *P. P.* were simultaneously increased, at a constant difference of 0.2 MPa, to 4.2 MPa and 4.0 MPa. The pressurized injection of methane gas into the unsaturated specimens began and methane gas gradually entered into the pore space. The temperature in the triaxial cell space was cooled to 1°C within the stability field of methane hydrate and the change of capillary water at grain contacts to methane hydrate initiated. The generation of methane hydrate lasted over a span from 24 h to 36 h under a prescribed pressure

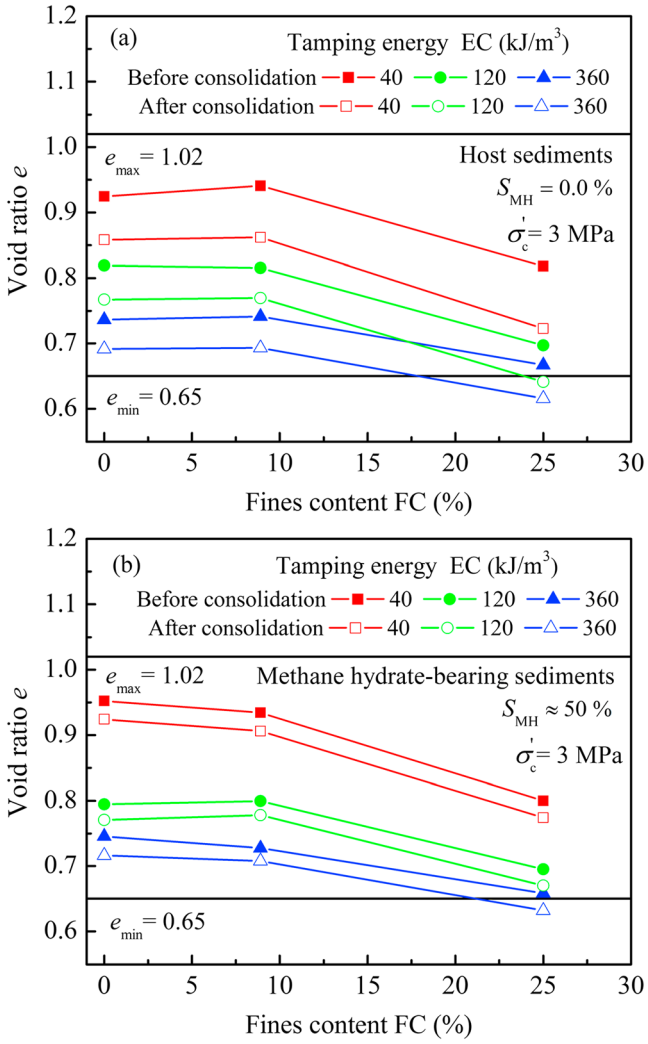

Figure 2. The variation in the void ratios of host sediments with different amounts of FC before and after isotropic consolidation loading. (a) Host sediments and (b) methane hydrate-bearing sediments.

and temperature path. No remarkable volume change in the upper and lower syringe pumps was the hint for the completion of methane hydrate formation.

2.3. Test Procedure and Conditions

Table 2 lists the triaxial compression test conditions on methane hydrate-bearing sediments with different amounts of FC. The cell pressure and pore pressure were gradually increased to 10.2 MPa and 10.0 MPa for all specimens after generation of methane hydrate. Subsequently, specimens were saturated by circulated pure water. It should be explained that cementing hydrate was initially formed at grain contacts in sediments using the partial water saturation method. The specimens were subsequently waterflooded prior to shearing for the purpose of saturation. Waterflooding the specimens moved a majority of hydrates initially formed at grain contacts into the pore space, producing load-bearing hydrate, and also weakened the cementing hydrate still remaining on sediment grains (Ebinuma et al., 2005). Besides, the nonuniform distributions of fines and water in unsaturated specimens led to the creation of heterogeneous hydrate. It was highly probable that the hydrate saturation was a combination of some weak cementation, mostly loading-bearing, partly heterogeneities in the specimens prepared in this study. The cell pressure and temperature were adjusted to the prescribed level. The specimens were isotropically consolidated until the desired effective confining pressure was attained. All triaxial compression tests were performed at an effective confining pressure of 3.0 MPa at constant strain rate, of 0.1%/m and terminated at axial strains of 30%. Methane hydrate was completely dissociated after the completion of shearing and the total amount of methane gas was measured by the gas mass flowmeter. The exact methane hydrate saturation S_{MH} was decided by the collected methane gas.

It is seen that actual methane hydrate saturation S_{MH} of each sample in Table 2 differs from the target value S_{MH} = 50%. A higher S_{MH} is probably due to newly formed hydrate synthesized from the circulated water and methane gas remaining in the pore space during the subsequent water saturation process. Priest et al. (2009) suggested that waterflooding a specimen created isolated gas bubbles that could be converted to load-bearing hydrate, meaning that hydrate may contact sediment grain surface if a large enough proportion formed. In the Priest et al. (2009) experiments, hydrate formed within the pore space between grains, probably at gas bubble-water interfaces, somewhere away from grain contacts and resulted in load-bearing hydrate. Hydrate formed during the waterflood in the present study is, by analogy, also the load-bearing hydrate which is the same as some of the existing hydrates in specimen that relocated and equilibrated during the waterflood. Accordingly, newly formed hydrate during the waterflood influences the shear strength of methane hydrate-bearing sediments in the same way as the main bulk of the hydrate in the specimen after the waterflood. A lower S_{MH} than 50% probably occurred because of dissolution of hydrates in the process of the waterflood and an initial reaction of less than the assumed initial water content. For the specimens with FC, the water may be pulled via capillary action into patches of high FC. Those water patches would only have easy access to methane on their outside surface, effectively limiting the overall surface area between water and gas during the hydrate formation stage, shielding water trapped within the patch of fines away from methane and leaving it unreacted and thus providing an overall lower hydrate saturation. From the authors' experiences, it is a significantly difficult task to keep the actual methane hydrate saturation exactly the same as the expected value in the experiments.

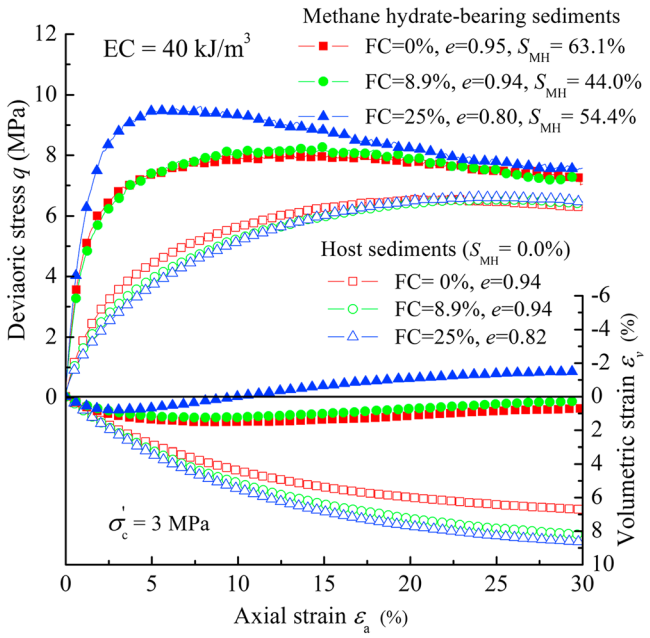

Figure 3. Stress-strain relationship of methane hydrate-bearing sediments and host sediments with different amounts of FC at loose state with tamping energy EC = 40 kJ/m^3.

3. Test Results

3.1. Void Ratios

Figure 2a shows the variation in the void ratios of host sediments with three amounts of FC and at three densities before and after isotropic consolidation loading. The maximum void ratio e_{max} of 1.02 and minimum void ratio e_{min} of 0.65 for clean host sands without FC are also shown. No remarkable variation in the void ratios of host sands is seen with a small amount of FC of 8.9% compared to clean host sands and a rapid decrement is noticed as the FC is increased to 25%. A possible explanation is that fines particles enter into the pore space and densify the specimens. Figure 2b presents the dependence of void ratio on FC for the corresponding methane hydrate-bearing sediments at three densities before and after isotropic consolidation loading. Void ratios of methane hydrate-bearing sediments tend to decrease as the amount of FC varies from 8.9% to 25%. Figures 2a and 2b reveal that an increase in tamping energy reduces the void ratios of all specimens prior to the formation of methane hydrate. All specimens subjected to isotropic confinement experience volume contraction and these give rise to the decline in void ratios. It is noted that the decrement of void ratios for methane hydrate-bearing sediments after isotopic consolidation is smaller than that of corresponding host sediments. The formation of methane hydrate in the pore space hinders the movement of grains and prompts compressive resistance strength. Void ratios of dense host sediments and the corresponding methane hydrate-bearing sediments with FC of 25% after consolidation are below the minimum void ratio determined for clean host sediments. This is because addition of fines particles into coarse-grained sand grains alters the maximum and minimum void ratios of mixtures. Such varying tendency has been pointed out by previous researchers (Lade & Yamamuro, 1997; Thevanayagam, 1998; Yang et al., 2006).

3.2. Stress-Strain Behavior

Figure 3 shows the deviatoric stress and volumetric strain plotted against the axial strain of methane hydrate-bearing sediments and hydrate-free sediments with three amounts of FC = 0%, 8.9%, and 25%, and at loose state with tamping energy EC = 40 kJ/m^3. The test results show that the presence of methane hydrate greatly increases peak shear strength and initial stiffness and prompts dilation tendency of methane hydrate-bearing sediments containing FC. This is consistent with previous experimental investigations on the synthetic methane hydrate-bearing sediments without FC and pressure core samples containing natural gas hydrate (Hyodo, Yoneda, et al., 2013; Masui et al., 2005; Miyazaki et al., 2011; Yoneda et al., 2015). The strengthening of sediments mainly originates from hydrate-occupied porosity and partially originates from intergranular strengthening stress which refers to weak bonding strength connecting the grains due to hydrate. All methane hydrate-bearing sediments exhibit initial strain-hardening followed by strain-softening behavior. Methane hydrate-bearing sediments rapidly gain their shear resistance at smaller axial strains and gradually lose shear strength after the peak value in accompaniment with the formation of a shear band. The rise in FC above 8.9% markedly increases peak deviatoric stress and intensifies dilation behavior of methane hydrate-bearing sediments. The hydrate-free sediments display strain-hardening behavior and attain their peak deviatoric stresses at larger strains. Increasing FC distinctively decreases the initial slope of stress-strain curve and increases volume contraction but has a minor effect on the peak shear strength.

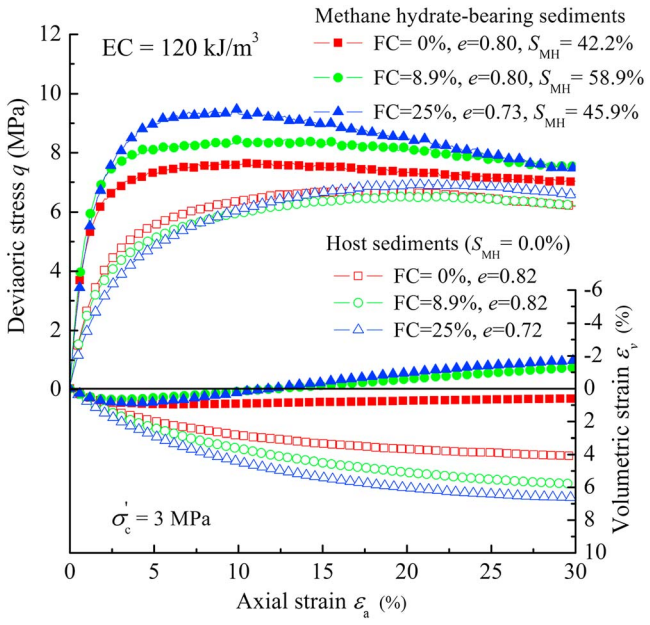

Figure 4. Stress-strain relationship of methane hydrate-bearing sediments and host sediments with different amounts of FC at medium-dense state with tamping energy EC = 120 kJ/m^3.

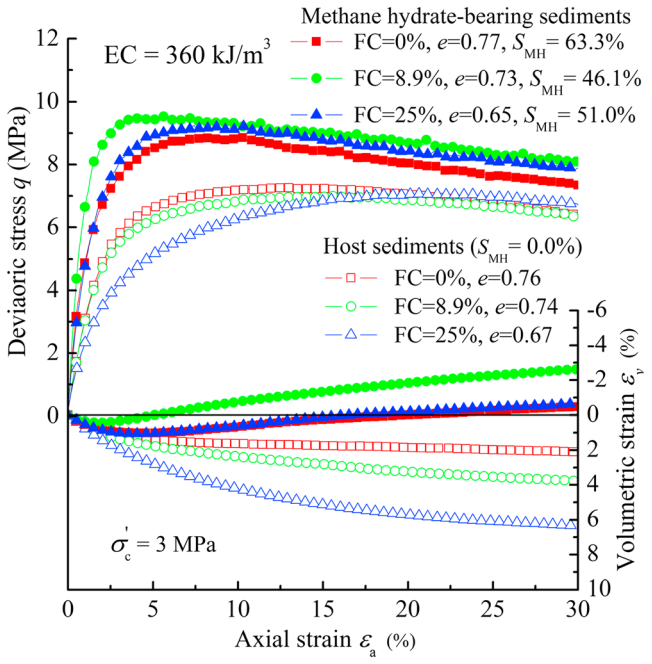

Figure 5. Stress-strain relationship of methane hydrate-bearing sediments and host sediments with different amounts of FC at dense state with tamping energy EC = 360 kJ/m^3.

Figure 4 presents the plot of deviatoric stress and volumetric strain against the axial strain of methane hydrate-bearing sediments and hydrate-free sediments with three amounts of FC and at medium-dense state with tamping energy EC = 120 kJ/m^3. Similar stress-strain curves are obtained to those in Figure 3, and different effects of FC on the variation in the geomechanical properties between methane hydrate-bearing sediments and hydrate-free sediments are also seen. In Figure 5, the relationship between the deviatoric stress, volumetric strain, and axial strain of densely packed methane hydrate-bearing sediments and host sediments with three amounts of FC and tamping energy EC = 360 kJ/m^3 is shown. The dependency of peak deviatoric stress and dilation on FC are less obvious for dense methane hydrate-bearing sediments. Marked dilation behavior is observed for all dense methane hydrate-bearing sediments with three amounts of FC. In the dense state, all host sands exhibit a slight postpeak strain-softening behavior. However, strain-hardening behavior of dense host sand remains and the specimen displays a smaller initial stiffness as the FC is increased to 25%. Obvious differences in the deviatoric stresses at the critical state (Been et al., 1991; Roscoe et al., 1963; Sadrekarimi & Olson, 2011; Santamarina & Cho, 2001) of methane hydrate-bearing sediments and hydrate-free sediments are observed in Figures 3–5. The critical state is an ultimate condition where a soil element will continue to deform without further change in stresses and volume (Schofield & Wroth, 1968). The entry of hydrate mass into the pore space and the creation of clusters of coarse-grained sand grains and fines particles with intergranular strengthening due to hydrate partially remaining at the critical state are believed to be the major factors leading to this difference.

To further understand the influence of density on the shear response of methane hydrate-bearing sediments and hydrate-free sediments, the results presented in Figures 3–5 are redrawn with FC = 0% (Figure 6), 8.9% (Figure 7), and 25% (Figure 8). The porosity represents the deposition history of the sediments in marine ground. A rise in density (tamping energy) enhances the peak deviatoric stress and initial stiffness of hydrate-free sediments and methane hydrate-bearing sediments with FC = 0% and 8.9%. Besides, densification of specimens also prompts dilation tendency of methane hydrate-bearing sediments and attenuates contraction tendency of host sediments. However, the influence of density on peak shear strength and initial stiffness enhancement diminishes when the addition of FC is 25%, as shown in Figure 8. For loose and dense sands containing a large amount of FC, pore spaces are prone to be extensively filled by fines particles. The overall shear strength and deformation behavior of methane hydrate-bearing sediments become less dependent on the density of coarse-grained sands once the amount of FC exceeds a certain value.

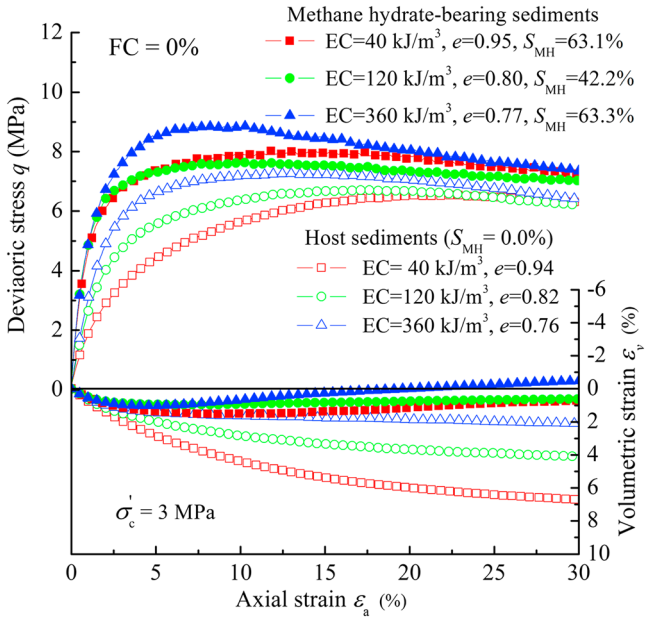

Figure 6. Stress-strain relationship of methane hydrate-bearing sediments and host sediments with FC = 0% at different densities.

4. Discussions

The influences of FC and density on peak shear strength, stiffness, and deformation behavior are further examined in this section.

4.1. Effects of Fines Content

Figure 9a shows the variation the in the peak deviatoric stresses q_{peak} of methane hydrate-bearing sediments and host sediments as a function of FC. The results imply that increasing FC within the range in this study improves the peak shear strength of methane hydrate-bearing

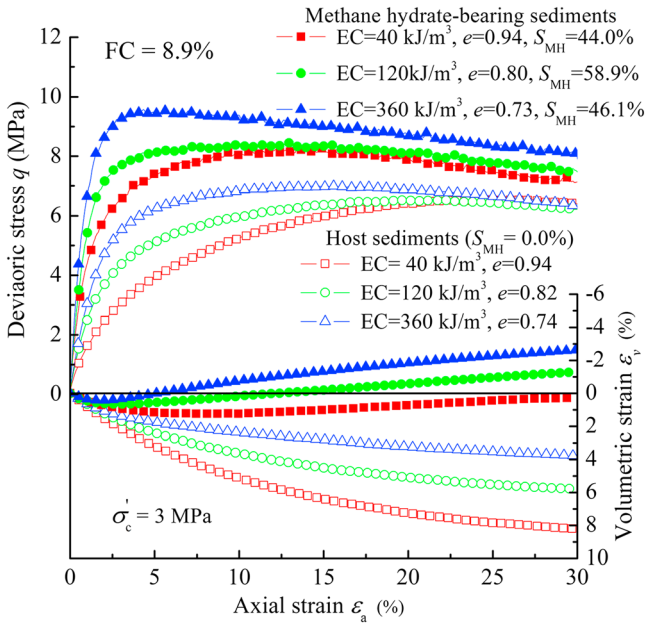

Figure 7. Stress-strain relationship of methane hydrate-bearing sediments and host sediments with FC = 8.9% at different densities.

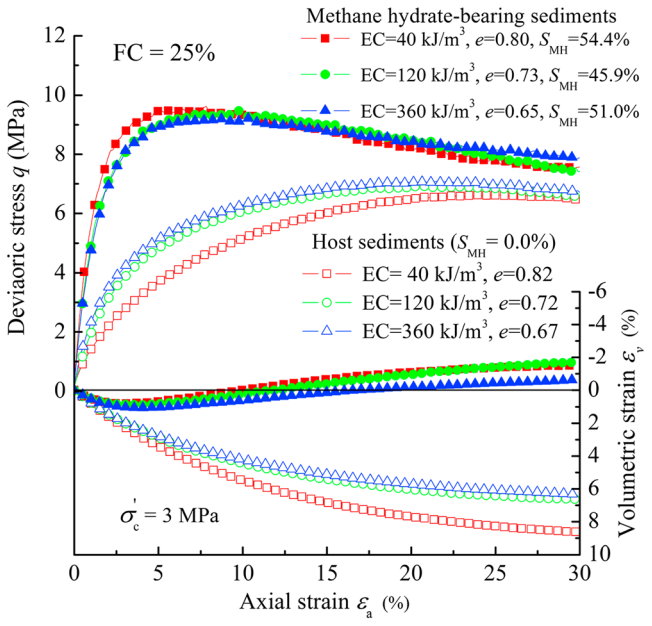

Figure 8. Stress-strain relationship of methane hydrate-bearing sediments and host sediments with FC = 25% at different densities.

sediments at loose and medium-dense states. This increasing tendency attenuates for densely tamped methane hydrate-bearing specimens. A rise in FC probably gives rise to the nonuniform distribution of fines and initially added water. The heterogeneous hydrates are likely to be created during methane hydrate formation. Bonded clusters of sand grains and fines particles held together by hydrate mass can be regarded as an associate unit during shearing due to the addition of fines particles. The creation of clusters of coarse-grained sand grains and fines particles with intergranular strengthening due to hydrate are considered as the primary reason for shear strength enhancement with the level of FC. Teerawattanasuk and Voottipruex (2014) studied the compression characteristics of fine-grained soil with various silty contents stabilized with cement and also pointed out that the yield strength increased with increasing silty content.

No remarkable change in the peak deviatoric stress of loose host sediments with EC = 40 kJ/m^3 is seen. Contrary to methane hydrate-bearing sediments, the peak deviatoric stress q_{peak} of dense host sediments with EC = 360 kJ/m^3 tends to slightly decrease with increasing FC. In terms of dense host sediments, fines particles initially fill the void space and increasing FC forces smaller fines particles to occupy contact locations between coarse-grained sand grains, further reducing the contact of coarse-grained sand grains. The fines particles act as lubricant and the structural rearrangement of sands containing FC slightly reduces the peak shear strength.

Figure 9b presents the dependence of the secant Young's modulus E_{50} of methane hydrate-bearing sediments and host sediments on FC. The secant Young's modulus E_{50} is determined using the expression $E_{50} = (q_{peak}/2)/\varepsilon_a$, where ε_a is the axial strain determined at half of the peak deviatoric stress. E_{50} proposed by Duncan and Chang (1970) was regarded as an important model parameter in describing the stress-strain curve of soils. E_{50} of methane hydrate-bearing sediments at loose state slightly increases with the rise in FC. However, varying tendency of E_{50} with the amount of FC begins to decline as EC is increased to 120 and 360 kJ/m^3. The E_{50} of host sediments exhibits a decreasing tendency as FC is increased. It can be seen that E_{50} of host sands increases from 2 to 6 times as much due to the formation of methane hydrate. The extent of enhancement is sensitive to the amounts of FC and density.

Figure 9c describes the variation in the dilation rates of methane hydrate-bearing sediments and hydrate-free sediments at the peak stress ratios $(d\varepsilon_v/d\varepsilon_a)_{peak}$ with different amounts of FC. The positive values for host sediments indicate the tendency toward contraction, while the negative values for methane hydrate-bearing sediments express expansion tendency. A rise in FC intensifies the varying tendencies of dilation rates of methane hydrate-bearing sediments and host sediments. Creation of bonded clusters with increasing FC further promotes dilation behavior. The variation in the deformation of methane hydrate-bearing sediments induced by the presence of methane hydrate had also been reported in previous investigations (Hyodo et al., 2005; Hyodo, Yoneda, et al., 2013; Masui et al., 2005; Miyazaki et al., 2011; Yoneda et al., 2015).

Figure 9d shows the stress ratios at the critical state η_{cs} of methane hydrate-bearing sediments and host sediments plotted against the FC. It is observed that the presence of methane hydrate markedly increases the stress ratios of specimens at the critical state. The stress ratios at the critical state increase with the rise in FC for methane

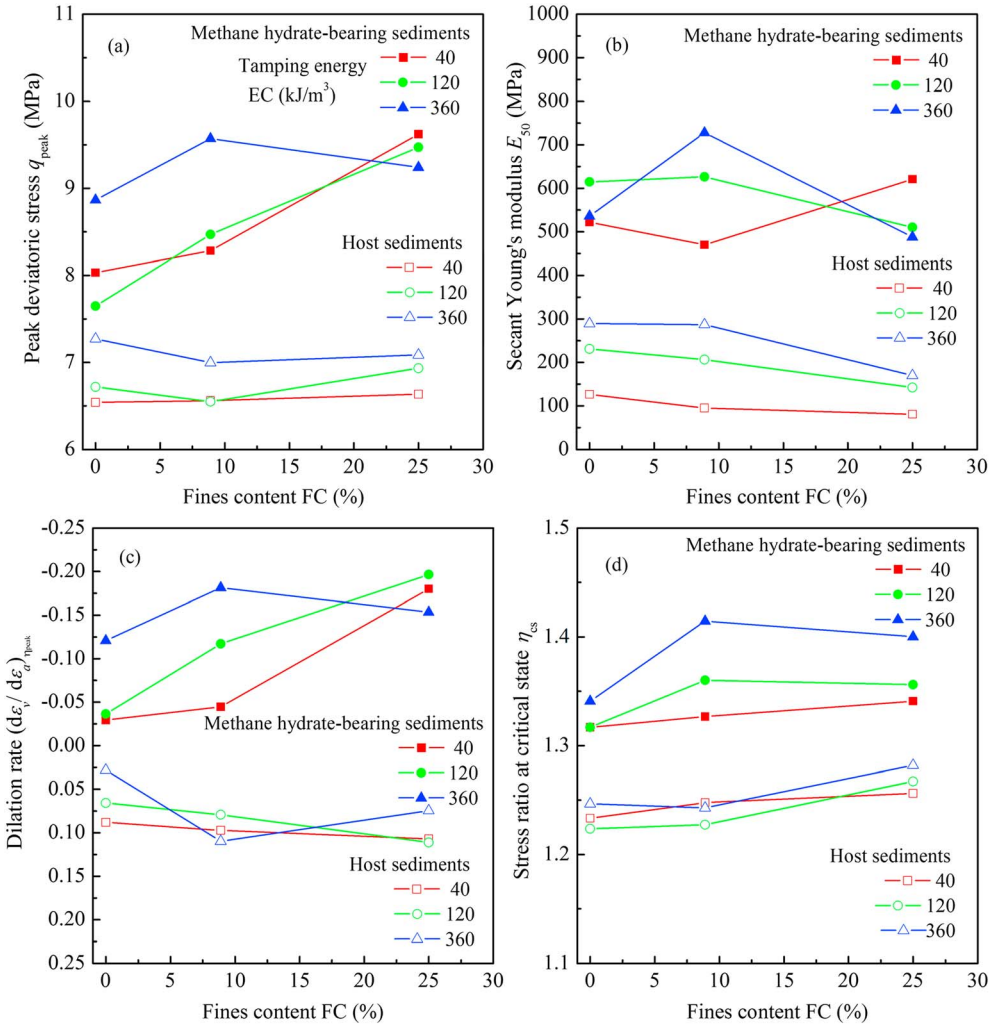

Figure 9. The strength and deformation parameters of methane hydrate-bearing sediments and host sediments with different amounts of FC (a) peak deviatoric stress q_{peak}, (b) secant Young's modulus E_{50}, (c) dilation rate at peak stress ratio $(d\varepsilon_v/d\varepsilon_a)_{\eta_{peak}}$, and (d) stress ratio at the critical state η_{cs}.

hydrate-bearing sediments. Partially unbroken clusters within samples and the entry of hydrate mass into the pore space give rise to the stress ratio increment at the critical state. Cruz, Rodrigues, and Viana da Fonseca (2011) studied the shear behavior of cemented sand with FC and also noticed a higher stress ratio at the critical state that was possibly related to the microfabric and cementation heterogeneities of tested samples. Wang and Leung (2008) studied the characterization of cemented sand and noted that the friction angle at the critical state was affected by the cement content. It was attributed to the existence of bonded clusters with a higher rolling resistance in the shear band at the ultimate state. The dependence of stress ratio on the hydrate saturation of hydrate-bearing sediments had also been reported by Jung et al. (2012) in their numerical investigations.

4.2. Effects of Void Ratio

Figure 10a presents the variation in the peak deviatoric stresses of methane hydrate-bearing sediments and host sediments at three densities. The results imply that the peak deviatoric stresses decrease with increasing void ratio with the exception of the methane hydrate-bearing sediment containing FC of 25%. A rise in the degree of compaction leading to the reduction of void ratio promotes dilation behavior and enhances shear resistance strength. Furthermore, the peak deviatoric stress of methane hydrate-bearing sediments positioned above those of host sediments is due to the presence of hydrate. Figure 10b shows that the secant

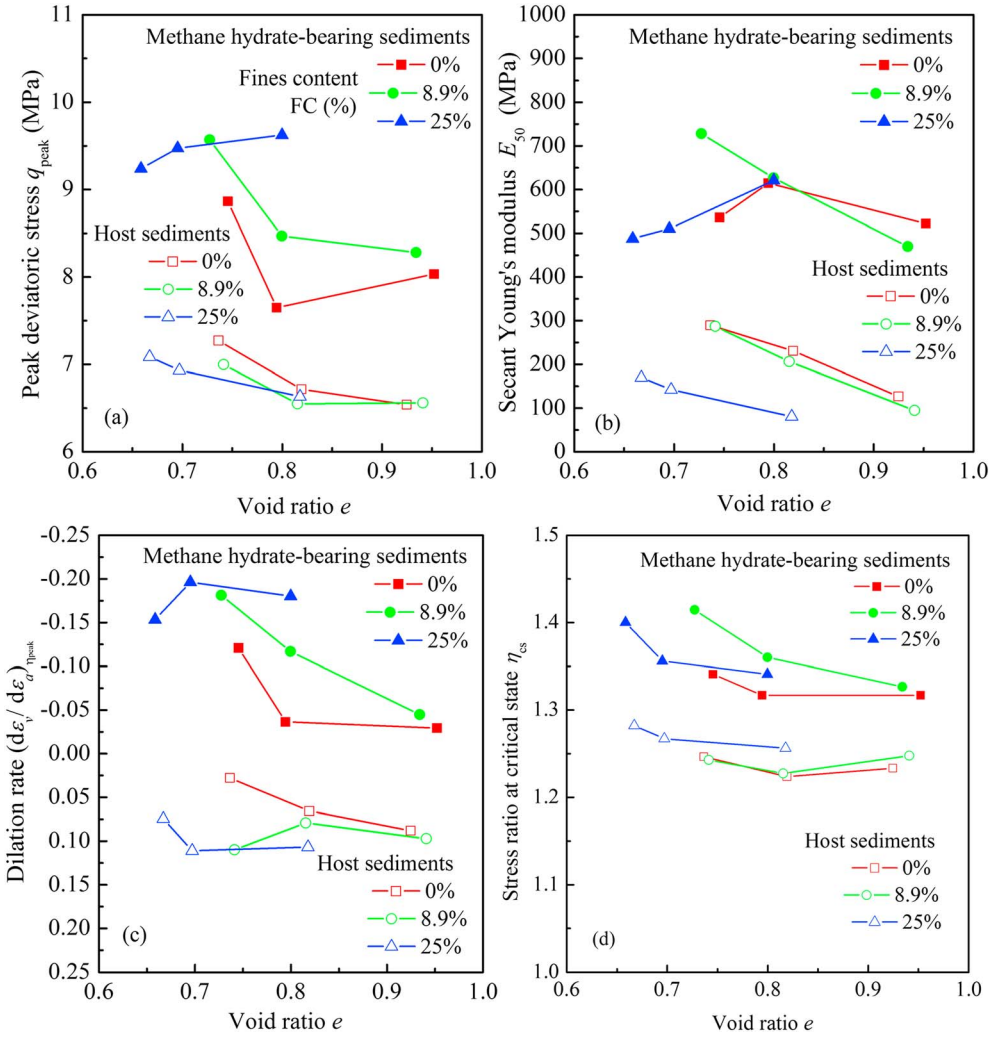

Figure 10. The strength and deformation parameters of methane hydrate-bearing sediments and host sediments at different levels of tamping energy EC (a) peak deviatoric stress q_{peak}, (b) secant Young's modulus E_{50}, (c) dilation rate at peak stress ratio $(d\varepsilon_v/d\varepsilon_a)_{\eta_{peak}}$, and (d) stress ratio at the critical state η_{cs}.

Young's modulus E_{50} tends to decrease with the rise in void ratios for methane hydrate-bearing sediments with FC of 0% and 8.9% and all host sediments. Figure 10c indicates that a reduction in void ratio intensifies dilation tendency of methane hydrate-bearing sediments and slightly attenuates the contraction tendency of hydrate-free sediments.

Figure 10d shows that the stress ratios at the critical state of methane hydrate-bearing sediments decrease with a rise in void ratio and this decreasing tendency is remarkable when the amount of FC is increased. The implication of these results is that the stress ratios at the critical state of methane hydrate-bearing sediments are sensitive to the amounts of FC and density. No obvious difference in the stress ratios at the critical state of host sediments at loose and medium-dense states is seen. The points representing the stress ratios at the critical state of methane hydrate-bearing sediments lie above those of host sediments. It had been previously interpreted that creation of bonded clusters was the major contributor to this difference.

4.3. Comparison of the Peak Shear Strength Between Methane Hydrate-Bearing Sediments With and Without FC

Figure 11 compares the variation in the peak deviatoric stresses q_{peak} of methane hydrate-bearing sediments with FC and without FC with the level of methane hydrate saturation under the same test conditions. The peak deviatoric stresses q_{peak} of methane hydrate-bearing sediments without FC hosted by silica sand

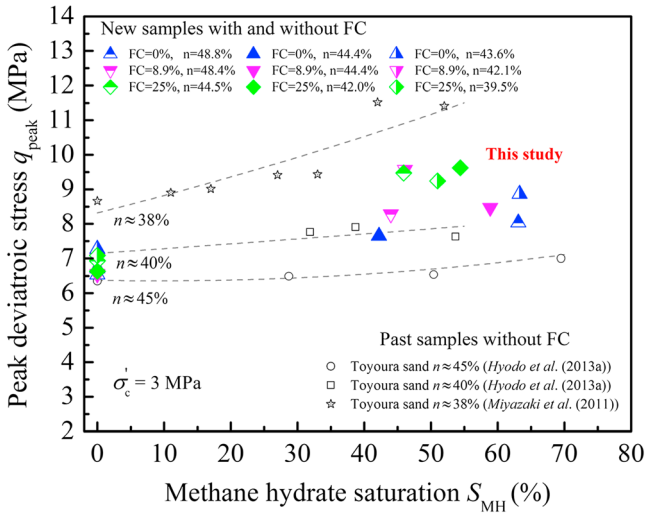

Figure 11. Comparison of the peak deviatoric stresses between methane hydrate-bearing sediments with and without FC.

with porosities n of 38%, 40%, and 45% at an effective confining pressure of 3.0 MPa are drawn in Figure 11 (Hyodo, Yoneda, et al., 2013; Miyazaki et al., 2011). For a specific porosity, the peak deviatoric stresses q_{peak} of methane hydrate-bearing sediments without FC tend to increase as methane hydrate saturation increases. To facilitate the comparison with previous data, the results of hydrate-free and methane hydrate-bearing sediment samples with various porosities tested in this study are shown with relatively larger symbols. It is distinctively seen that the solid symbols representing the peak deviatoric stresses q_{peak} of methane hydrate-bearing sediments with FC of 0%, 8.9%, and 25% lie above the trend lines of the peak deviatoric stresses q_{peak} of previously measured methane hydrate-bearing sediments without FC, but with similar porosity. This is probably because that bonded clusters are liable to be created for sediments with FC. Bonded clusters prevent the force-chain buckling and thus improve peak shear strength. The peak deviatoric stresses q_{peak} of methane hydrate-bearing sediments at a given effective confining pressure are a complex function of the amount of FC, density, and methane hydrate saturation.

It is also noted that the peak deviatoric stresses q_{peak} from past results are dependent on the density (porosity) of specimens and increase with decreasing porosity. In exception of the density effect, the larger difference between the shear strength measured by Miyazaki et al. (2011) with porosity of 38% and the results reported by Hyodo, Yoneda, et al. (2013) with porosity of 40% was also originated from the implementation order of consolidation and hydrate formation. Miyazaki et al. (2011) consolidated their specimens before hydrate formation, and the specimens were likely to end up with more of load supported by sediment grains. Hyodo, Yoneda, et al. (2013) initially conducted the consolidation and subsequently accomplished the hydrate formation. Thus, specimens prepared by Miyazaki et al. (2011) had a stronger sediment frame and an additional strengthening by undeformed hydrate to start the shear test even at a similar density. Additionally, the load cell of the triaxial apparatus employed by Miyazaki et al. (2011) was installed outside the cell and took into account the piston friction. The inclusion of piston friction in measured results also led to a greater shear strength.

4.4. Mechanism Controlling the Shear Behavior of Methane Hydrate-Bearing Sediments With and Without FC

Figure 12 presents the hypothetical microstructure image of samples to interpret the mechanisms controlling the shear behavior of methane hydrate-bearing sediments and hydrate-free sediments with a small and large amount of FC and without FC at a grain-scale viewpoint. The composition of a clean, hydrate-free sample assembled of sand grains and a hydrate-free mixture sample composed of sand grains and fines particles are shown in the left portion. For specimens with a small amount of FC, fines particles fall into the void space between coarse-grained sand grains. For specimens containing a large amount of FC, fines particles partially fill the void space and partially separate the contacts of coarse-grained sand grains (Carraro et al., 2009; Santamarina & Jang, 2009; Thevanayagam et al., 2002). Such microstructure of sand-silty mixture reduces the void ratio in Figure 2 and postpones the appearance of peak shear strength but minimally affects its magnitude in Figures 3–5.

The middle portion of Figure 12 describes the initial hydrate formation pattern formed in coarse-grained sands with different amounts of FC and without FC in advance of waterflooding the specimens in sample preparation stage. In terms of host sands without FC and with a small amount of FC, hydrates are formed at the menisci between grains and firmly cement the neighboring grains. For the host sands containing FC, the existence of FC and the rise in the amount of FC can facilitate the creation of larger bonded clusters of sand grains and fines particles with intergranular strengthening due to hydrate.

In the right portion of Figure 12, waterflooding moves a majority of hydrates initially formed at grain contacts into the pore space. Some hydrates likely still remain at sediment grain contacts but the cementing effect is extensively weakened. It is highly probable that the mixed modes of load-bearing hydrate, weaken cementing hydrate, and heterogeneous hydrate are produced. The hydrate mass existing in the pore space bridges

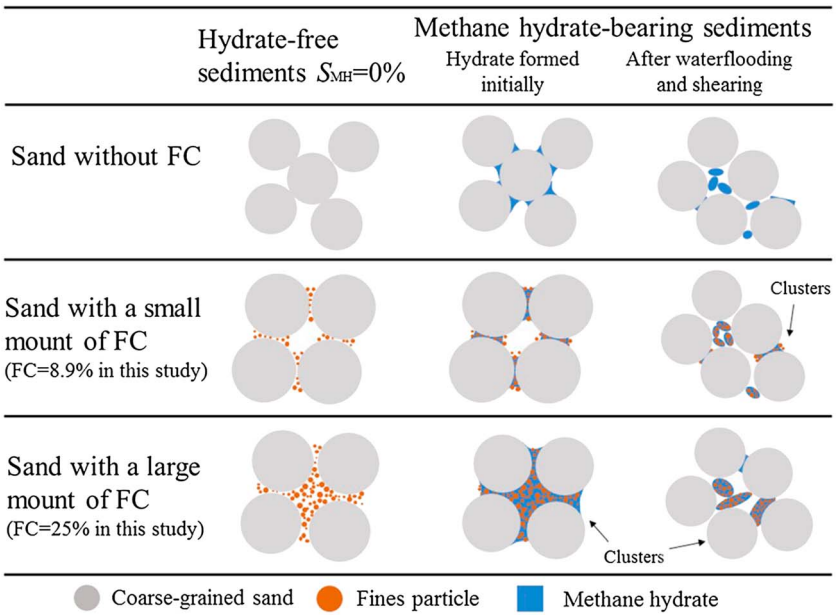

Figure 12. Grain-scale mechanisms controlling the shear strength of methane hydrate-bearing sediments with a small and larger amount of FC and without FC.

the neighboring grains and strengthens the granular skeleton by joining the load-bearing work (Waite et al., 2009). These load-bearing hydrates interact with the surrounding sediment grains and restrict the buckling of "force chains," further intensifying the microscale dilation behavior and shear strength enhancement. For specimens with FC, nonuniform distributions of fines and water produce a heterogeneous hydrate distribution, such as bonded clusters. A rise in FC probably increases the number and size of heterogenous hydrates, and their interactions would sustain a higher shear strength. These clusters still partially remain at larger shear strains, and they give rise to the stress ratio increment at the critical state for methane hydrate-bearing sediments with FC. Wang and Leung (2008) commented that the force chains involved to sustain the loading at the critical state may contain more clusters, creating a larger rolling resistance at grain contacts in cemented sand. Accordingly, the existence, spatial distribution, and amount of FC affect hydrate formation patterns as well as the interparticle interaction between sand grains.

5. Conclusions

A series of triaxial compression tests were performed on methane hydrate-bearing sediments and their corresponding hydrate-free sediments with different amounts of FC and at three densities to examine their influences on geomechanical properties. The effect of FC on the shear response of methane hydrate-bearing sediments was interpreted at a grain-scale viewpoint. Moreover, a comparative analysis of peak deviatoric stress was also made between methane hydrate-bearing sediments with and without FC under the same test conditions. The major conclusions of this study are summarized as follows:

1. The amount of FC greatly affects the void ratios of specimens prior to the formation of hydrate. The initial void ratios tend to decrease with increasing FC at each level of density. An explanation is that fines particles enter into the void space and densify the specimens. The decrease in void ratios of methane hydrate-bearing sediments during consolidation is smaller than that observed in hydrate-free sediments. The formation of methane hydrate in the pore space hinders the deformation and movement of grains and prompts the compressive resistance strength of samples.
2. The presence of methane hydrate in specimens alters the stress-strain curves from strain-hardening to postpeak strain-softening behavior and the volumetric strain from contraction to dilation at a given amount of FC and level of density.
3. The existence of FC plays different roles in the shear response of methane hydrate-bearing sediments and hydrate-free sediments. The addition of FC greatly enhances the shear strength and promotes dilation

behavior of methane hydrate-bearing sediments. It is noted that such an effect of FC is prominent at loose state. In contrast, a rise in FC delays the appearance of the peak shear strength, significantly reduces initial stiffness, and increases contractive behavior of hydrate-free sediments.

4. A rise in tamping energy applied to the specimen increases the peak shear strength and initial stiffness and promotes dilation behavior of hydrate-free sediments with three amounts of FC and methane hydrate-bearing sediments containing FC of 0% and 8.9%. The effect of density on the shear response of methane hydrate-bearing sediment with FC of 25% is not clear and becomes minimal.
5. The stress ratios at the critical state of methane hydrate-bearing sediments are higher than those of hydrate-free sediments. This is attributed to the entry of hydrate into the pore space between sand grains and the formation of bonded clusters of hydrate, sand, and fines. Additionally, clusters of coarse-grained sand grains and fines particles with intergranular strengthening due to hydrate partially remain even when the specimen enters into the critical state.

These results are expected to be employed to obtain a deep understanding of the mechanical properties of methane hydrate-bearing sediments containing FC and to propose a constitutive model considering the effects of FC in subsequent studies. Also, the presence of FC on the mechanical properties of methane hydrate-bearing sediments during hydrate dissociation is particularly relevant and requires examination in further investigations.

Acknowledgments

The authors would gratefully like to acknowledge the support provided by the Research Consortium for Methane Hydrate Resources in Japan (MH21 Research Consortium) as planned by the Ministry of Economy, Trade, and Industry (METI), Japan, and Japan Society for the Promotion of Science under the Grant-in-Aid for Scientific Research (A) 25249065 and Grants-in-Aid for JSPS Fellows 15F15368. The data for this paper are available by contacting the corresponding author at yang-wuuu0226@hotmail.com. The authors wish to express their sincere thanks to the people concerned. The authors would like to thank William F Waite and another anonymous reviewer and the Associate Editor for their comments and suggestions for improving the quality of this study.

References

Been, K., Jefferies, M. G., & Hachey, J. (1991). The critical state of sands. *Géotechnique*, *41*(3), 365–381. https://doi.org/10.1680/geot.1991.41.3.365

Brugada, J., Cheng, Y. P., Soga, K., & Santamarina, J. C. (2010). Discrete element modelling of geomechanical behaviour of methane hydrate soils with pore-filling hydrate distribution. *Granular Matter*, *12*(5), 517–525. https://doi.org/10.1007/s10035-010-0210-y

Carraro, J. A. H., Prezzi, M., & Salgado, R. (2009). Shear strength and stiffness of sands containing plastic or nonplastic fines. *Journal of Geotechnical and Geoenviromental Engineering*, *135*(9), 1167–1178. https://doi.org/10.1061/(ASCE)1090-0241(2009)135:9(1167)

Chong, Z. R., Yang, S. H. B., Babu, P., Linga, P., & Li, X.-S. (2015). Review of natural gas hydrates as an energy resource: Prospects and challenges. *Applied Energy*, *162*, 1633–1652. https://doi.org/10.1016/j.apenergy.2014.12.061

Cruz, N., Rodrigues, C., & Viana da Fonseca, A. (2011). The influence of cementation in the critical state behaviour of artificial bonded soils. In *International symposium on deformation characteristics of geomaterials* (pp. 730–737). Seoul, Korea: IOS Press.

Dai, S., Santamarina, J. C., Waite, W. F., & Kneafsey, T. J. (2012). Hydrate morphology: Physical properties of sands with patchy hydrate saturation. *Journal of Geophysical Research: Solid Earth*, *117*, B11205. https://doi.org/10.1029/2012JB009667

Duncan, J. M., & Chang, C.-Y. (1970). Nonlinear analysis of stress and strain in soils. *Journal of the Soil Mechanics and Foundations Division*, *96*(5), 1629–1653.

Durham, W. B., Kirby, S. H., Stern, L. A., Zhang, W., Durham, W. B., Kirby, S. H., … Zhang, W. (2003). The strength and rheology of methane clathrate hydrate. *Journal of Geophysical Research: Solid Earth*, *108*(B410), B4. https://doi.org/10.1029/2002JB001872

Ebinuma, T., Kamata, Y., Minagawa, W., Ohuma, R., Nagao, J., & Narita, H. (2005). Mechanical properties of sandy sediment containing methane hydrate. In *Proceeding of the 5h Int. Conf. on Gas Hydrate* (pp. 958–961). Trondheim, Norway: Tapir Academic Press.

Egawa, K., Nishimura, O., Izumi, S., Fukami, E., Jin, Y., Kida, M., … Nakatsuka, Y. (2015). Bulk sediment mineralogy of gas hydrate reservoir at the East Nankai offshore production test site. *Marine and Petroleum Geology*, *66*, 379–387. https://doi.org/10.1016/j.marpetgeo.2015.02.039

Englezos, P. (1993). Review: Clathrate hydrates. *Industrial and Engineering Chemistry Research*, *32*(7), 1251–1274. https://doi.org/10.1021/ie00019a001

Fujii, T., Nakamizu, M., Tsuji, Y., Kawasaki, M., & Ochiai, K. (2005). Modes of occurrence and accumulation mechanism of methane hydrate-result of MET1 exploration test wells "tokai-oki to kumanonada". In *Proceeding of the 5h Int. Conf. on Gas Hydrate* (pp. 974–979). Trondheim, Norway.

Grozic, J., & Ghiassian, H. (2010). Undrained shear strength of methane hydrate-bearing sand; preliminary laboratory results. In *Proceeding of 6th Canadian Permafrost Conference and 63rd Canadian Geotechnical Conference* (pp. 459–466). Calgary, Canada.

Hyodo, M., Li, Y., Yoneda, J., Nakata, Y., Yoshimoto, N., Nishimura, A., & Song, Y. (2013). Mechanical behavior of gas-saturated methane hydrate-bearing sediments. *Journal of Geophysical Research: Solid Earth*, *118*, 5185–5194. https://doi.org/10.1002/2013JB010233

Hyodo, M., Nakata Y., & Yoshimoto, N. (2015). Challenge for methane hydrate production by geotechnical engineering. In *Proceeding of the 15th Asian Regional Conference on Soil Mechanics and Geotechnical Engineering* (pp. 62–75). Fukuoka, Japan.

Hyodo, M., Nakata, Y., Yoshimoto, N., & Ebinuma, T. (2005). Basic research on the mechanical behavior of methane hydrate-sediments mixture. *Soils and Foundations*, *45*(1), 75–85.

Hyodo, M., Wu, Y., Kajiyama, S., Nakata, Y., & Yoshimoto, N. (2017). Effect of fines on the compression behaviour of poorly graded silica sand. *Geomechanics and Engineering*, *12*(1), 127–138. https://doi.org/10.12989/gae.2017.12.1.127

Hyodo, M., Yoneda, J., Yoshimoto, N., & Nakata, Y. (2013). Mechanical and dissociation properties of methane hydrate-bearing sand in deep seabed. *Soils and Foundations*, *53*(2), 299–314. https://doi.org/10.1016/j.sandf.2013.02.010

Ito, T., Komatsu, Y., Fujii, T., Suzuki, K., Egawa, K., Nakatsuka, Y., … Nagao, J. (2015). Lithological features of hydrate-bearing sediments and their relationship with gas hydrate saturation in the eastern Nankai Trough, Japan. *Marine and Petroleum Geology*, *66*, 368–378. https://doi.org/10.1016/j.marpetgeo.2015.02.022

Jin, G., Xu, T., Xin, X., Wei, M., & Liu, C. (2016). Numerical evaluation of the methane production from unconfined gas hydrate-bearing sediment by thermal stimulation and depressurization in Shenhu area, South China Sea. *Journal of Natural Gas Science and Engineering*, *33*, 497–508. https://doi.org/10.1016/j.jngse.2016.05.047

Jung, J. W., Santamarina, J. C., & Soga, K. (2012). Stress-strain response of hydrate-bearing sands: Numerical study using discrete element method simulations. *Journal of Geophysical Research: Solid Earth*, *117*, B04202. https://doi.org/10.1029/2011JB009040

Kajiyama, S., Hyodo, M., Nakata, Y., Yoshimoto, N., Wu, Y., & Kato, A. (2017). Shear behaviour of methane hydrate bearing sand with various particle characteristics and fines. *Soils and Foundations*, *57*(2), 176–193. https://doi.org/10.1016/j.sandf.2017.03.002

Kajiyama, S., Wu, Y., Hyodo, M., Nakata, Y., Nakashima, K., & Yoshimoto, N. (2017). Experimental investigation on the mechanical properties of methane hydrate-bearing sand formed with rounded particles. *Journal of Natural Gas Science and Engineering*, *45*, 96–107. https://doi.org/10.1016/j.jngse.2017.05.008

Kleinberg, R. L., Flaum, C., Griffin, D. D., Brewer, P. G., Malby, G. E., Peltzer, E. T., & Yesinowski, J. P. (2003). Deep sea NMR: Methane hydrate growth habit in porous media and its relationship to hydraulic permeability, deposit accumulation, and submarine slope stability. *Journal of Geophysical Research: Solid Earth*, *108*(B10), B10. https://doi.org/10.1029/2003JB002389

Kneafsey, T. J., Tomutsa, L., Moridis, G. J., Seol, Y., Freifeld, B. M., Taylor, C. E., & Gupta, A. (2007). Methane hydrate formation and dissociation in a partially saturated core-scale sand sample. *Journal of Petroleum Science and Engineering*, *56*(1–3), 108–126. https://doi.org/10.1016/j.petrol.2006.02.002

Kvenvolden, K. A. (1995). A review of the geochemistry of methane in natural gas hydrate. *Organic Geochemistry*, *23*(11–12), 997–1008. https://doi.org/10.1016/0146-6380(96)00002-2

Lade, P. V., & Yamamuro, J. A. (1997). Effects of nonplastic fines on static liquefaction of sands. *Canadian Geotechnical Journal*, *34*(6), 918–928. https://doi.org/10.1139/t97-052

Li, X.-S., Xu, C.-G., Zhang, Y., Ruan, X.-K., Li, G., & Wang, Y. (2016). Investigation into gas production from natural gas hydrate: A review. *Applied Energy*, *172*, 286–322. https://doi.org/10.1016/j.apenergy.2016.03.101

Lin, J.-S., Seol, Y., & Choi, J. H. (2015). An SMP critical state model for methane hydrate-bearing sands. *International Journal for Numerical and Analytical Methods in Geomechanics*, *39*(9), 969–987. https://doi.org/10.1002/nag.2347

Makogon, Y. F. (2010). Natural gas hydrates—A promising source of energy. *Journal of Natural Gas Science and Engineering*, *2*(1), 49–59. https://doi.org/10.1016/j.jngse.2009.12.004

Masui, A., Haneda H., Ogata Y., & Aoki K. (2005). Effects of methane hydrate formation on shear strength of synthetic methane hydrate sediments. In Proceeding of the 5th International Conference on Gas Hydrates (ICGH 2005) (pp. 364–369). Trondheim, Norway.

METI (2005). *Mid-Term Evaluation Report of the Japan's Methane Hydrate R&D Program*. Tokyo, Japan.

Minagawa, H., Nishikawa, Y., Ikeda, I., Miyazaki, K., Takahara, N., Sakamoto, Y., … Nairta, H. (2008). Characterization of sand sediment by pore size distribution and permeability using proton nuclear magnetic resonance measurement. *Journal of Geophysical Research: Solid Earth*, *113*, B07210. https://doi.org/10.1029/2007JB005403

Miyazaki, K., Masui, A., Sakamoto, Y., Aoki, K., Tenma, N., & Yamaguchi, T. (2011). Triaxial compressive properties of artificial methane-hydrate-bearing sediment. *Journal of Geophysical Research: Solid Earth*, *116*, B06102. https://doi.org/10.1029/2010JB008049

Miyazaki, K., Tenma, N., Aoki, K., & Yamaguchi, T. (2012). A nonlinear elastic model for triaxial compressive properties of artificial methane-hydrate-bearing sediment samples. *Energies*, *5*(10), 4057–4075. https://doi.org/10.3390/en5104057

Ning, F., Yu, Y., Kjelstrup, S., Vlugt, T. J. H., & Glavatskiy, K. (2012). Mechanical properties of clathrate hydrates: Status and perspectives. *Energy and Environmental Science*, *5*(5), 6779. https://doi.org/10.1039/c2ee03435b

Nixon, M. F., & Grozic, J. L. (2007). Submarine slope failure due to gas hydrate dissociation: A preliminary quantification. *Canadian Geotechnical Journal*, *44*(3), 314–325. https://doi.org/10.1139/t06-121

Pauli, C. K., Ussler, W., & Dillon, W. P. (2003). Potential role of gas hydrate decomposition in generating submarine slope failures. In M. D. Max (Ed.), *Natural gas hydrate: In oceanic and permafrost environments* (pp. 149–156). Dordrecht, Netherlands: Springer.

Pinkert, S., Grozic, J. L. H., & Priest, J. A. (2013). Strain-softening model for hydrate-bearing sands. *International Journal of Geomechanics*, *15*(6), 4015007. https://doi.org/10.1061/(ASCE)GM.1943-5622.0000477

Priest, J. A., Best, A. I., & Clayton, C. R. I. (2006). Attenuation of seismic waves in methane gas hydrate-bearing sand. *Geophysical Journal International*, *164*(1), 149–159. https://doi.org/10.1111/j.1365-246X.2005.02831.x

Priest, J. A., Druce, M., Roberts, J., Schultheiss, P., Nakatsuka, Y., & Suzuki, K. (2015). PCATS Triaxial: A new geotechnical apparatus for characterizing pressure cores from the Nankai Trough, Japan. *Marine and Petroleum Geology*, *66*, 460–470. https://doi.org/10.1016/j.marpetgeo.2014.12.005

Priest, J. A., Rees, E. V. L., & Clayton, C. R. I. (2009). Influence of gas hydrate morphology on the seismic velocities of sands. *Journal of Geophysical Research: Solid Earth*, *114*, B11205. https://doi.org/10.1029/2009JB006284

Roscoe, K. H., Schofield, A. N., & Thurairajah, A. (1963). Yielding of clays in states wetter than critical. *Géotechnique*, *13*(3), 211–240. https://doi.org/10.1680/geot.1963.13.3.211

Sadrekarimi, A., & Olson, S. M. (2011). Critical state friction angle of sands. *Géotechnique*, *61*(9), 771–783. https://doi.org/10.1680/geot.9.P.090

Sakamoto, Y., Masayo, K., Miyazaki, K., Tenma, N., Komai, T., Yamaguchi, T., … Ohga, K. (2009). Numerical study on dissociation of methane hydrate and gas production behavior In Laboratory-Scale Experiments For Depressurization: Part 3—Numerical Study On Estimation of Permeability In Methane Hydrate Reservoir. *International Journal of Offshore and Polar Engineering*, *19*(2), 1–11.

Sánchez, M., Gai, X., & Santamarina, J. C. (2017). A constitutive mechanical model for gas hydrate bearing sediments incorporating inelastic mechanisms. *Computers and Geotechnics*, *84*, 28–46. https://doi.org/10.1016/j.compgeo.2016.11.012

Santamarina, J., & Cho, G. (2001). Determination of critical state parameters in sandy soils—Simple procedure. *Geotechnical Testing Journal*, *24*(2), 185–192. https://doi.org/10.1520/GTJ11338J

Santamarina, J. C., & Jang, J. (2009). Gas production from hydrate bearing sediments: Geomechanical implications. *DOE-NETL Fire Ice*, *9*(4), 18–22.

Santamarina, J. C., Dai, S., Terzariol, M., Jang, J., Waite, W. F., Winters, W. J., … Suzuki, K. (2015). Hydro-bio-geomechanical properties of hydrate-bearing sediments from Nankai Trough. *Marine and Petroleum Geology*, *66*, 434–450. https://doi.org/10.1016/j.marpetgeo.2015.02.033

Schofield, A. N., & Wroth, C. P. (1968). *Critical state soil mechanics*. New York, NY: McGraw-Hill.

Scholz, N. A., Riedel M., Spence G. D., Hyndman R. D., James T., Naegeli K., … Hamilton T. (2011). Do dissociating gas hydrates play a role in triggering submarine slope failures? A case study from the northern Cascadia margin. In *The 7th International Conference on Gas Hydrates (ICGH 2011)* (pp. 1–8). Edinburgh, Scotland, United Kingdom.

Shen, J., Chiu, C. F., Ng, C. W. W., Lei, G. H., & Xu, J. (2016). A state-dependent critical state model for methane hydrate-bearing sand. *Computers and Geotechnics*, *75*, 1–11. https://doi.org/10.1016/j.compgeo.2016.01.013

Shen, Z., & Jiang, M. (2016). DEM simulation of bonded granular material. Part II: Extension to grain-coating type methane hydrate bearing sand. *Computers and Geotechnics*, *75*, 225–243. https://doi.org/10.1016/j.compgeo.2016.02.008

Sloan, E. D. J. (1998). Gas hydrates: Review of physical/chemical properties. *Energy & Fuels*, *12*(2), 191–196. https://doi.org/10.1021/EF970164+

Sloan, E. D., & Koh, C. A. (2007). *Clathrate hydrates of natural gases* (3rd ed.). Boca Raton, FL: CRC Press.
Sultan, N., Marsset, B., Ker, S., Marsset, T., Voisset, M., Vernant, A. M., … Drapeau, D. (2010). Hydrate dissolution as a potential mechanism for pockmark formation in the Niger delta. *Journal of Geophysical Research: Solid Earth*, *115*, B08101. https://doi.org/10.1029/2010JB007453
Suzuki, K., Ebinuma, T., & Narita, H. (2009). Features of methane hydrate-bearing sandy-sediments of the forearc basin along the Nankai Trough: Effect on methane hydrate-accumulating mechanism in turbidite. *Journal of Geography (Chigaku Zasshi)*, *118*(5), 899–912. https://doi.org/10.5026/jgeography.118.899
Teerawattanasuk, C., & Voottipruex, P. (2014). Influence of clay and silt proportions on cement-treated fine-grained soil. *Journal of Materials in Civil Engineering*, *26*(3), 420–429. https://doi.org/10.1061/(ASCE)MT.1943-5533.0000813
Thevanayagam, S. (1998). Effect of fines and confining stress on undrained shear. *Journal of Geotechnical and Geoenviromental Engineering*, *124*(6), 479–491. https://doi.org/10.1061/(ASCE)1090-0241(1998)124:6(479)
Thevanayagam, S., Shenthan, T., Mohan, S., & Liang, J. (2002). Undrained fragility of clean sands, silty sands, and sandy silts. *Journal of Geotechnical and Geoenviromental Engineering*, *128*(10), 849–859. https://doi.org/10.1061/(ASCE)1090-0241(2002)128:10(849)
Trehu, A. M., Long, P. E., Torres, M. E., Bohrmann, G. R. R. F., Rack, F. R., Collett, T. S., … Bangs, N. L. (2004). Three-dimensional distribution of gas hydrate beneath southern Hydrate Ridge: Constraints from ODP Leg 204. *Earth and Planetary Science Letters*, *222*(3–4), 845–862. https://doi.org/10.1016/j.epsl.2004.03.035
Uchida, S., Soga, K., & Yamamoto, K. (2012). Critical state soil constitutive model for methane hydrate soil. *Journal of Geophysical Research: Solid Earth*, *117*, B03209. https://doi.org/10.1029/2011JB008661
Waite, W. F., Winters, W. J., & Mason, D. H. (2004). Methane hydrate formation in partially water-saturated Ottawa sand. *American Mineralogist*, *89*(July), 1202–1207. https://doi.org/10.2138/am-2004-8-906
Waite, W. F., Santamarina, J. C., Cortes, D. D., Dugan, B., Espinoza, D. N., Germaine, J., … Soga, K. (2009). Physical properties of hydrate-bearing sediments. *Reviews of Geophysics*, *47*, RG4003. https://doi.org/10.1029/2008RG000279
Wang, Y. H., & Leung, S. C. (2008). Characterization of cemented sand by experimental and numerical investigations. *Journal of Geotechnical and Geoenviromental Engineering*, *134*(7), 992–1004. https://doi.org/10.1061/(ASCE)1090-0241(2008)134:7(992)
Winters, W. J., Waite, W. F., Mason, D. H., Gilbert, L. Y., & Pecher, I. A. (2007). Methane gas hydrate effect on sediment acoustic and strength properties. *Journal of Petroleum Science and Engineering*, *56*(1–3), 127–135. https://doi.org/10.1016/j.petrol.2006.02.003
Xu, W., & Germanovich, L. N. (2006). Excess pore pressure resulting from methane hydrate dissociation in marine sediments: A theoretical approach. *Journal of Geophysical Research: Solid Earth*, *111*, B01104. https://doi.org/10.1029/2004JB003600
Xu, M., Song, E., Jiang, H., & Hong, J. (2016). DEM simulation of the undrained shear behavior of sand containing dissociated gas hydrate. *Granular Matter*, *18*(4), 1–13. https://doi.org/10.1007/s10035-016-0675-4
Yang, S. L., Sandven, R., & Grande, L. (2006). Steady-state lines of sand–silt mixtures. *Canadian Geotechnical Journal*, *43*(11), 1213–1219. https://doi.org/10.1139/t06-069
Yoneda, J., Masui, A., Konno, Y., Jin, Y., Egawa, K., Kida, M., … Tenma, N. (2015). Mechanical properties of hydrate-bearing turbidite reservoir in the first gas production test site of the Eastern Nankai Trough. *Marine and Petroleum Geology*, *66*, 471–486. https://doi.org/10.1016/j.marpetgeo.2015.02.029
Yu, Y., Cheng, Y. P., Xu, X., & Soga, K. (2016). Discrete element modelling of methane hydrate soil sediments using elongated soil particles. *Computers and Geotechnics*, *80*, 397–409. https://doi.org/10.1016/j.compgeo.2016.03.004
Yun, T. S., Santamarina, C. J., & Ruppel, C. (2007). Mechanical properties of sand, silt, and clay containing tetrahydrofuran hydrate. *Journal of Geophysical Research: Solid Earth*, *112*, B04106. https://doi.org/10.1029/2006JB004484